Boron Nitride Nanotubes Filled with Ni and $NiSi_2$ Nanowires in Situ

Chengchun Tang,*,† Yoshio Bando,† Dmitri Golberg,† Xiaoxia Ding,‡ and Shouren Qi‡

Advanced Materials Laboratory, National Institute for Materials Science, 1-1 Namiki, Tsukuba, Ibaraki 305-0044, Japan, and Department of Physics, Central China Normal University, China

Received: February 5, 2003; In Final Form: April 28, 2003

An in situ synthesis method to fill boron nitride (BN) nanotubes with metals or metal alloys was proposed using a vapor−liquid−solid catalytic growth mechanism. Nickel fillings could be obtained by using nickel foil or a silicon substrate covered with nickel film during catalytic growth of pure BN nanotubes. The filled nickel nanowires usually connect to nanoparticles at the tip-end of BN nanotubes. Extensive structural investigations display the general existence of 4-fold superstructures along the [100] and [110] axes. The superstructures ensure the existence of one set of {223} planes of the cubic nickel parallel to the BN sheet, its planar distance are four times the interplanar spacing of the BN nanotubes shell, and the Ni−Ni distance in this plane is equal to the B−B and N−N distance. The (223) plane grows directly on the (0002) plane of the BN tubular layer according to a lattice-match relationship between the BN shell and the cubic nickel. $NiSi_2$ nanowires could also fill BN nanotubes when using a silicon substrate covered with a nickel film. The alloy nanowires have the growth axis along the [0−11] direction and the (−422) planes grow parallel to the innermost BN shells. The grown plane has the three times planar distance of the BN (0002) shells, and the atomic distance in this plane accords with B−B and N−N bonds. All the results indicate that metal Ni and $NiSi_2$ crystallizes on the innermost shell of the BN nanotubes at a specified plane restricted by the all-space lattice-match relationship. Investigations further confirm the nanometallurgical behavior: crystallization of liquid metals is strongly confined by BN nanotube geometry.

Introduction

Extensive research on boron nitride (BN) nanotubes has immediately followed the discovery of carbon nanotubes.[1−4] In view of the structural similarity of graphite and hexagonal BN, it is common to discuss morphologies and formation mechanisms of BN nanotubes in terms of some models designed for carbon nanotubes. However, BN nanotubes exhibit unique physical and chemical properties that are considerably different than carbon nanotubes. The electronic properties of carbon nanotubes may range from metallic to semiconducting with the strong dependence on chirality and diameter, while BN nanotubes exhibit relatively uniform semiconducting behavior with a wide band gap weakly dependent on geometrical configuration.[5] In addition, in contrast to the intense chemical reduction nature of carbon, graphite-like BN is quite stable, even at high temperature and in harsh environment. The chemical inertness displayed by BN nanotubes has been reported.[6] Considering that a nanometer scale will probably accelerate the oxidation of some metallic nanowires, a feasible strategy has been suggested to use BN nanotubes as protecting "cages" or "molds" for any metallic material encapsulated within.[7]

Metals and/or metal compounds filling carbon nanotubes via chemical methods has been reported. The methods allow carbon nanotubes to be opened at the tip-ends and filled with some specific materials having low surface tension via capillary and wet-chemical actions.[8−10] However, to date there has been limited success in analogous filling of BN nanotubes using chemical methods,[11] partly due to difficulties in tip-opening and/or wetting of BN nanotubes. We have noticed that a high-temperature growth method, using composite metal−carbon electrodes during arc vaporization, has been used to fill carbon nanotubes with various metals or metallic compounds.[12] The crystallization of encapsulated materials and the growth of carbon nanotubes are strongly coupled due to the chemical reaction between the tube and the metallic material. Therefore, carbon nanotubes could be filled with several pure metals and metallic carbides. However, clues with respect to filling of BN nanotubes may be obtained from the high-temperature growth process: simultaneously introducing metals during growth of BN nanotubes, which overcomes the difficulties of consecutive tip-opening and wetting of BN nanotubes.

In fact, randomly formed metal-based nanoparticles were observed in the tips of BN nanotubes synthesized via arc discharge or laser ablation with metal−boron electrodes.[1,2] Invar Fe−Ni alloy nanorods also filled BN nanotubes during high-temperature conversion of carbon nanotubes with metal encapsulations to BN nanotubes.[13] BN nanotubes filled with SiC nanorods were prepared using the similar carbon-nanotube-confined reaction methods.[14] Very recently, we reported the BN coating of SiC nanowires through simultaneous growth of BN and SiC in the presence of Ni−C catalysts.[15] All mentioned experiments imply that the high-temperature simultaneous growth procedure should be a feasible strategy to achieve a large-scale filling of BN nanotubes with metals.

In addition, to avoid the formation of metal carbides, attention should be paid to carbon incorporation during the proposed high-temperature, simultaneous growth process for metal-filling of BN nanotubes.[16] Fortunately, some successes have been achieved in carbon-free growing of BN nanotubes.[17−19] Recently, a novel

* To whom correspondence should be addressed. E-mail: Tang.Chengchun@nims.go.jp.

† National Institute for Materials Science.

‡ Central China Normal University.

10.1021/jp034310q CCC: $25.00
Published on Web 06/14/2003

precursor, the mixture of boron monoxide and magnesium which are in-situ generated by reacting boron and magnesium oxide at high temperature, has been utilized to effectively synthesize bulk amounts of carbon-free pure BN nanotubes.[20]

In this paper, we report a synthetic route to successfully fill BN nanotubes with nickel nanowires at a high yield. We also demonstrated that BN nanotubes may serve as a one-dimensional chemical reactor exhibiting nanometallurgical behavior when filled with Ni and $NiSi_2$ nanowires.

Experimental Section

All chemical reagents were bought from Aldrich with the purity of 99.995% for amorphous boron powder and 99% for magnesium oxide powder. The mixture of boron and magnesium oxide powders with a molar ratio of 1:1 was thoroughly mixed by ball-milling for 6 h and was then used as the reactant to in-situ generate the vapor precursors of BN nanotubes at a high temperature of 1300 °C.

A piece of 1 mm thick nickel foil and a (100) single-crystal silicon wafer with approximately 300 nm thickness nickel film were used as the substrate to deposit BN nanotubes. Before use, the nickel foil and silicon wafer were rinsed in distilled water, degreased in acetone, and etched in a dilute hydrogen fluoride solution for a few seconds. The pretreatment processes could reduce the oxide thickness on the silicon substrates and form a rough surface on the nickel foil. Nickel deposition on silicon substrate was performed for 4 h by a RF sputtering system in a multicycled mode at a rate of 1.5 nm/min. The as-sputtered film was annealed at 500 °C for 3 h in flowing argon to form a strongly adhered nickel layer.

A RF induction furnace was used to synthesize the BN nanotubes with metal nanowires fillings. The substrate and the mixture of boron−magnesia were put into a long BN boat, which was placed into a graphite susceptor in an induction furnace. A temperature gradient of 200 °C was kept between the mixture source and the substrates when the mixture was heated to 1300 °C by adjusting the locations of reacting crucibles. The experimental setup and vapor flow directions are schematically shown in Figure 1. Argon was used as a carrier gas to transport the simultaneously generated boron monoxide and magnesium vapors. The argon flow was maintained at 30 standard cubic centimeters per minute (sccm) during reaction. When the substrate was heated to 1100 °C, ammonia gas was introduced at a flow rate of 200 sccm and flowed over the substrate. After 100 min of transport reaction, the ammonia flow was shut off and the furnace was gradually cooled to room temperature. The products were scraped from the substrates.

The crystal structure and chemical composition of the products were examined by means of X-ray powder diffraction. The morphologies of the as-synthesized samples were analyzed by scanning electron microscopy (SEM, JEOL, JSM-6700F). Sample powders removed from the substrates were also ultrasonically dispersed in CCl_4 solution and dropped onto a carbon-coated copper grid for analysis by means of a high-resolution field emission transmission electron microscope (TEM, JEOL, JEM-3000F) operated at 300 kV. Energy-dispersive X-ray analysis (EDX) and electron energy loss (EEL) spectroscopy with a stationary focused 0.5 nm electron probe were employed to identify the elemental compositions of the tubes and the encapsulated nanowires.

Results and Discussion

The deposited material on the nickel foil does not strongly adhere and is peeled off easily, while the deposition on silicon substrate exhibits somewhat strong adhesion. XRD measurements indicate that a face-centered cubic nickel could be detected from the samples collected both from the nickel foil and the silicon substrate. It is worth noting that the crystalline $NiSi_2$ with cubic CaF_2 structure can also be formed in the product on the silicon substrate. We therefore suggest that the following metallurgical process occurs near the surface of silicon substrate:

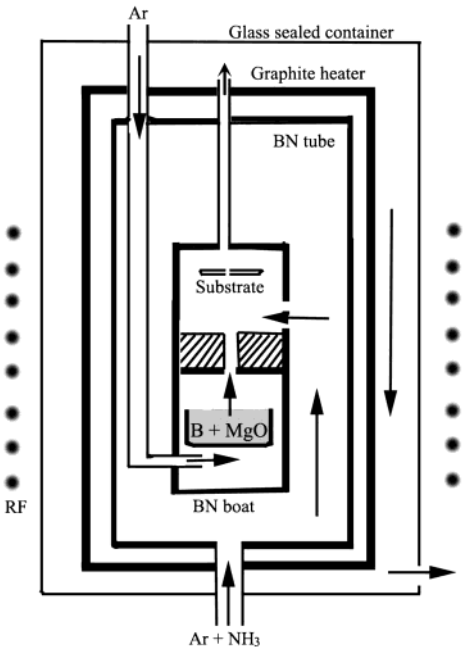

Figure 1. Schematic of the fillings of BN nanotubes. The arrows show the directions of the gas flows. Nickel foil and silicon substrate (covered with 300 nm thick nickel film) were put into the chamber, where the reaction temperature is adjusted to 1100 °C, when the mixed reactant was heated to 1300 °C. Samples were collected from the surfaces of the nickel foil and silicon substrate.

$$Ni + 2Si \rightarrow NiSi_2 \quad (1)$$

The SEM image shown in Figure 2a depicts the morphology of the product scraped from the nickel foil. A significant fraction of bright contrast objects could be observed, which are attributed to the images from metal nickel. Although nickel particles were attached to the surface of BN nanotubes, we also observed metal nickel inside BN nanotubes to form the encapsulated nanoparticles or nanowires. The BN nanotubes grown on the silicon substrate display similar nickel attachments and fillings (Figure 2b).

Due to the high vapor pressure at the deposition temperature of 1100 °C, magnesium could not be confined geometrically by the BN nanotubes during the growth process, as described in our previous growth research on BN nanotubes.[20] We also observed some white BN attached at the inner wall of reaction chamber. SEM and TEM characterizations show that the sample exhibits the structure similar to the BN nanotubes without introducing the substrate.

For the sample deposited on the nickel foil, the observed fillings only result from metal nickel (Figure 3a). Over 80% of the BN nanotubes were filled, as estimated from more than 100 tubes by our TEM examinations. The filled BN nanotubes usually display different morphologies, which consist of either nanoparticles encapsulated within the tip-ends of BN nanotubes or long continuous nanowires in BN nanotubes. The longest filling reaches several hundred nanometers. Some nickel nano-

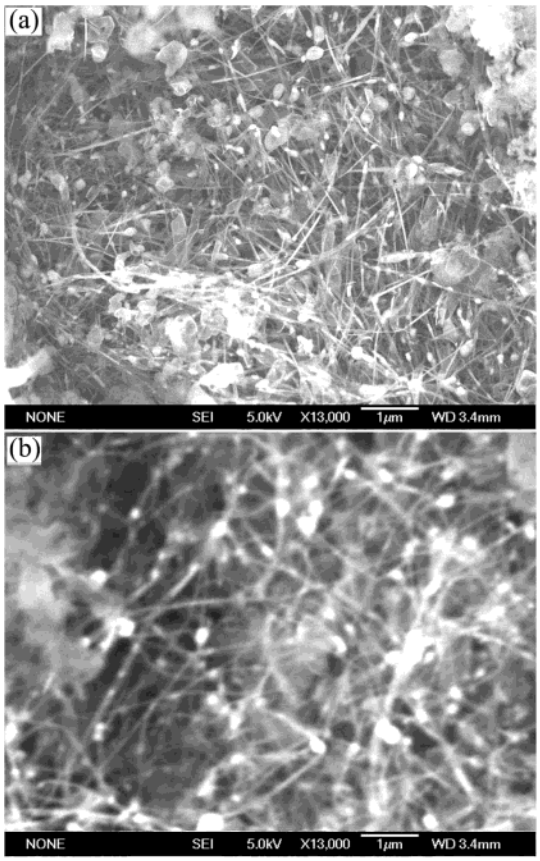

Figure 2. SEM images showing the morphologies of the products. (a) The sample taken from the surface of nickel foil: metal nanoparticles or nanowires (bright contrast area in the figure) are encapsulated in the nanotubes; some large-diameter BN whiskers could also be found. (b) The sample on the silicon substrate: the nanotubes grown from the substrate exhibit the same filling morphology.

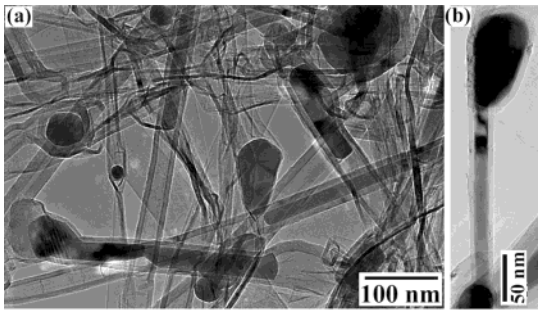

Figure 3. TEM images of the samples in the presence of nickel. (a) The filling Ni nanowires are usually join with the tip-ending nanoparticles. (b) A Ni nanowire connects to two nanoparticles.

particles not directly attached to the tube ends of BN nanotubes could also be observed. They typically join the tip-ending nanoparticle through a continuous nanowire. This morphology is shown in Figure 3b. Isolated nickel nanowires not attached to the nanoparticles were rarely observed. We can also find BN nanotubes with nickel fillings with the similar morphologies in the product collected from the surface of the silicon substrate covered with nickel film.

High-resolution TEM and selected area electron diffraction (SAED) analyses were used to further investigate the structural orientation relationships between the Ni fillings and the BN nanotubes. Figure 4 shows the typical features of the Ni fillings. A Ni-filled BN nanotube attaches to a Ni nanoparticle at a BN tube end and is ~55 nm in diameter (Figure 4a). No high-symmetry atomic planes that are parallel to the BN shell could

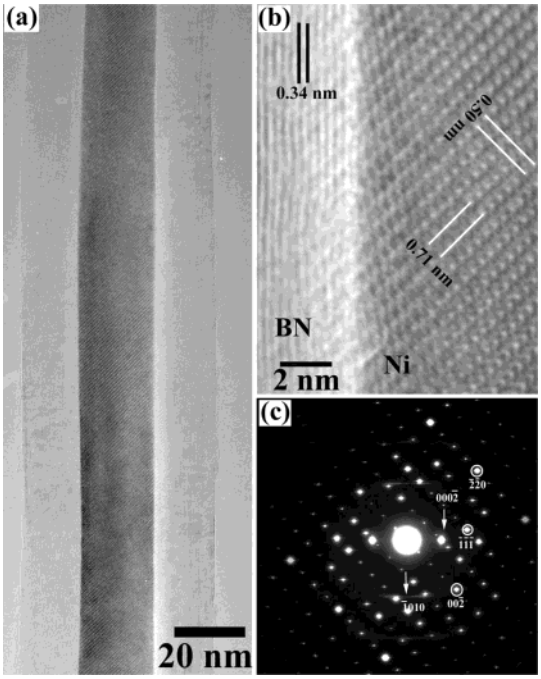

Figure 4. (a) Structural analyses of Ni-filled BN nanotubes. (b) High-resolution TEM image showing the existence of a 4-fold superstructure. (c) SAED pattern. Here the arrows point to the reflections from the BN tubes, whereas a circle marks the reflection from cubic Ni.

be found from the high-resolution TEM image (Figure 4b), while two well-ordered crystalline planes with the spacing of 0.50 and 0.71 nm could be clearly observed. The planar distances correspond to four times the distances of the (220) plane (0.1246 nm) and the (200) plane (0.1762 nm) of cubic nickel, indicating the existence of a 4-fold superstructure.

The corresponding SAED pattern (Figure 4c) clearly shows the superstructure and orientation relationships. The diffraction pattern of the BN nanotubes (marked with the arrows) is characteristic of the nearly zigzag arrangement (the [−1010] direction is nearly parallel to the tube axis). The high-intensity spots on the diffraction pattern originating from the Ni nanowires form a rectangular array, consistent with the face-centered cubic [−110] zone axis of nickel. The 4-fold superstructure reflections along the [100] and [011] directions could be observed clearly; therefore, the superperiodicity along the two directions is equal to 4 times the planar distances and relies on the 4-fold superstructure in the above high-resolution TEM image. In fact, all our electron diffraction observations on the filled Ni nanowires confirmed the general existence of this 4-fold superstructure.

The growth direction of nickel nanowires along the BN shell stands between the [111] and [113] directions and is approximately normal to the {223} plane of superstructural Ni in the [−110] direction. It is worth noting that one of the nearest distances in the {223} planes is equal within 0.003 nm to the B−B and N−N distance (0.249 nm) along the zigzag edge of the BN sheet. Additionally, the planar distance of Ni(223) is 0.08515 nm, which is equal to 0.25 times of the layer spacing of BN(0002) (0.33) within 0.0006 nm. Considering the existence of the superstructure along the [100] and [110] directions, the diffractions of the (223) planes could be observed due to the close lattice match between the Ni(223) plane and h-BN(0002) plane, as highlighted in the SADP pattern. The spatial lattice-match relationship controls the epitaxial recrystallization of Ni on the innermost BN graphite-like layer.

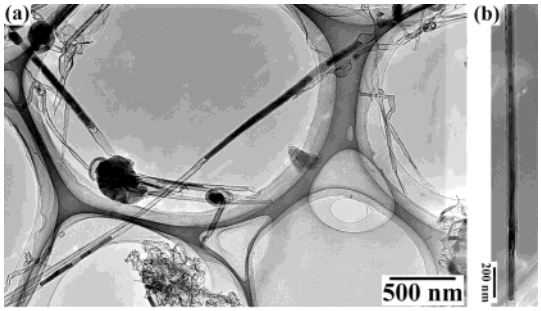

Figure 5. (a) The filled $NiSi_2$ nanowires usually do not attach to the nanoparticles. (b) The $NiSi_2$ nanowire fillings usually exhibit the longer filled length than Ni nanowire filling, the longest of which reaching several micrometers.

Although the Ni-filled BN nanotubes can be found in the sample from the surface of silicon substrate, the more commonly observed filling composition is $NiSi_2$ phase, which can be confirmed by the extensive EDX analyses for the filled metals with a constant molar ratio between Ni and Si approaching 1:2 (Ni:Si). This result is in agreement with the observation of XRD. A significant share of fillings exists in the middle of BN nanotubes and usually do not attach to the nanoparticles. A typical filling morphology is shown in Figure 5a. In addition, the $NiSi_2$ nanowires usually have a larger filled length than Ni nanowires, the longest of which reaches several micrometers (Figure 5b).

Different than fillings of metal Ni, the $NiSi_2$ fillings show a slightly different superstructure. Figure 6 depicts the filling feature of $NiSi_2$ nanowires in the middle of BN nanotubes and without the attachment to a nanoparticle. The filled nanotube discussed here is 44 nm in diameter, and the diameter of Ni nanowires is approximately 20 nm (Figure 6a). A SAED pattern taken from the filled alloy nanowires could be indexed as a [111] zone axis (Figure 6b). Figure 6c shows the diffraction pattern obtained through tilting the specimen around the zone axis, indicating the zigzag arrangement of the outer BN nanotube.[21] The BN tube (0002) plane is approximately parallel to one set of the $NiSi_2\{422\}$ planes. The superstructure reflections along the $NiSi_2\{220\}$ planes display a 2-fold symmetry. Although we could not obtain a good quality SAED pattern showing the superperiodicity along the [112] direction, a 3-fold symmetry should be expected on the basis of the orientation rule obtained in the case of Ni fillings. Spacing that is 3 times that of the (422) planes (0.1105 nm) is in a good agreement with the distance of the BN shell (0.33 nm). The Ni−Si bond length on the planes coincides with the nearest B−B or N−N distance.

The filled $NiSi_2$ nanowires grow along the [110] direction and the direction of the epitaxial crystallization on the BN shell is [112]. The high-resolution TEM image of the filled tube (Figure 6d) confirms the morphology and superstructure mentioned above. On the basis of the above-mentioned orientation correlation, we believe that filling with Ni and $NiSi_2$ takes place simultaneously with the growth of the BN nanotubes. The binary phase diagram of the Ni−Si system[22] indicates that a Si rich Ni−Si alloy is in the liquid phase at the deposition temperature of 1100 °C. The liquid Ni−Si alloy could catalytically grow BN nanotubes within a vapor−liquid−solid growth mechanism and also might be absorbed into the as-formed BN nanotube to form an encapsulated nanowire. The nanowire length strongly depends on the amount of Ni or Ni−Si solution located near the starting growth point. Although the bulk metal nickel is still in a solid state at the deposition temperature, the size effect of the melting point dependence for nanomaterials[23] ensures the

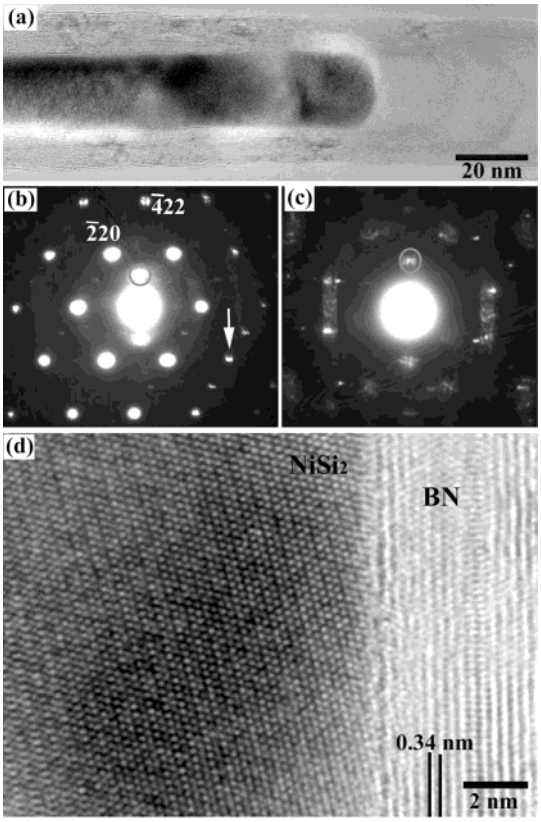

Figure 6. Structural analyses of $NiSi_2$ fillings. (a) TEM image of the $NiSi_2$-filled BN nanotubes. (b) SAED pattern taken along the [111] zone axis; a circle points to the BN (0002) planes and an arrow marks the 2-fold superstructural reflection along the [110] direction. (c) SAED pattern taken away from the zone axis obtained by tilting the sample, showing the zigzag arrangement of the tubular shell. (d) High-resolution TEM image displaying the superstructure and the growth orientation.

occurrence of some liquid-phase nickel at the rough surface of the nickel foil. The acid pretreatment procedure for the nickel foil creates some nanoscale nickel particles on the foil. This should be the reason that $NiSi_2$ has the longer filled length and can exist in the middle of nanotubes—there is more liquid Ni−Si alloys than nanoscale liquid Ni at the deposited area.

During the cooling process, the filled liquid substances crystallize in the BN nanotubes. Obviously, the crystalline structures of the filled substances strongly depend on the morphology of BN nanotubes. The epitaxial recrystallization process in the BN nanotubes could be further confirmed by extensive TEM observations. Figure 7a shows a filled Ni nanowire separated by a short hollow space. It is interesting to point out that the fragment morphologies adjacent to the hollow space obviously exhibit a symmetric geometry. Considering that the thermal expansion coefficient of metal Ni is nearly 20 times larger than the in-plane expansion coefficient of the hexagonal BN, the volume shrinkage is more severe for the Ni filling than for BN sheets. Therefore, it is reasonable to assume that two fragments were separated from a continuous liquid-phase Ni filling during cooling. For $NiSi_2$ nanowire filling, the $NiSi_x$ alloy particles embedded in $NiSi_2$ nanowires could be frequently observed, as shown in Figure 7b. The EDX patterns taken from the dark contrast area and from the uniform nanowire are shown in Figure 7c,d. The composition analyses clearly indicate the existence of $NiSi_x$ and $NiSi_2$. Taking into account that the Ni−Si alloy is in a liquid phase at the Ni/Si concentration ranging from 0.5 to 1.5,[22] the $Ni_{1+x}Si_2$ ($0 < x < 2$) might be absorbed into the BN nanotubes. During cooling, the growth of $NiSi_2$ nanowires excludes the excess liquid from forming

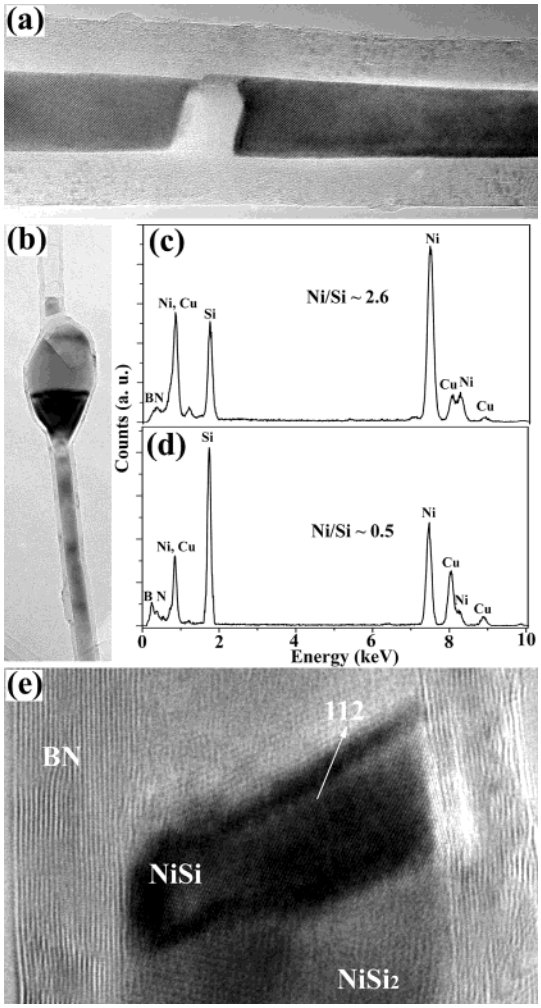

Figure 7. Nanometallurgical behavior inside BN nanotubes. (a) A filling Ni nanowire separated by a short hollow space, and the two fragments exhibit a symmetric geometry. (b) The $NiSi_x$ alloy particles embedded in the $NiSi_2$ nanowires and the EDX patterns taken from the dark contrast area and the uniform nanowires, indicating the existence of (c) $NiSi_{\sim 0.4}$ and (d) $NiSi_2$. (e) The high-resolution TEM image of an orthorhombic NiSi alloy precipitation at the end of the $NiSi_2$ nanowire.

$NiSi_x$ alloy particles. The precipitated $NiSi_x$ usually occurs at the end of the filled alloy nanowires. Figure 7e shows the high-resolution TEM image of an orthorhombic NiSi alloy precipitation at the end of the $NiSi_2$ nanowire.

All the results clearly indicate the nanometallurgical behavior inside BN nanotubes: crystallization of metals inside the nanosized volume confined by a nanotubular shape. For the $NiSi_2$ case, the macroeutectic reaction[22]

$$L \leftrightarrow NiSi + \alpha NiSi_2 \quad (56.2-66.7 \text{ at. \% Si concentration, } 966\ ^\circ C) \quad (2)$$

should also take place during the so-called nanometallurgical process. However, due to the lattice-match confinement from the BN template, only $NiSi_2$ could be formed in continuous nanowires, but $NiSi_x$ forms in the nanoparticle precipitate.

Summary

We reported the in-situ filling of BN nanotubes with cubic metal Ni and $NiSi_2$ nanowires and the electron microscopic study of the resultant structures and defects. The BN nanotube fillings clearly exhibit nanometallurgical behavior: the absorbed liquid metals crystallize in BN nanotubes and grow parallel to the innermost tube shell. The confinement from the lattice-match relationship between the BN shell and the filled metals results in the possible growth of specific alloy phases.

Acknowledgment. The authors thank Dr. F. F. Xu, Dr. Z. W. Liu, Dr. G. Movelell, and Dr. Y. Akahane, for helpful discussions on TEM characterization, and Dr. T. Sato and Dr. Y. Uemura, for the support of this research. Authors acknowledge the financial support from NSFC (Grant No. 50202007).

References and Notes

(1) Chopra, N. G.; Luyren, R. J.; Cherry, K.; Crespi, V. H.; Cohen, M. L.; Louie, S. G.; Zettl, A. *Science* **1995**, *269*, 966.

(2) Loiseau, A.; Williaime, F.; Demoncy, N.; Hug, G.; Pascard, H. *Phys. Rev. Lett*. **1996**, *76*, 4737.

(3) Terrones, M.; Hsu, W. K.; Terrones, H.; Zhang, J. P.; Ramos, S.; Hare, J. P.; Castillo, R.; Prassides, K.; Cheetham, A. K.; Kroto, H. W.; Walton, D. R. M. *Chem. Phys. Lett*. **1996**, *259*, 568.

(4) Golberg, D.; Bando, Y.; Eremets, M.; Takemura, K.; Kurashima, K.; Tamiya, K.; Yusa, H. *Chem. Phys. Lett*. **1997**, *279*, 191. Tang, C. C.; Bando, Y.; Ding, X. X.; Qi, S. R.; Golberg, D. *J. Am. Chem. Soc*. **2002**, *124*, 14550.

(5) Rubio, A.; Corkill, J. L.; Cohen, M. L. *Phys. Rev. B* **1994**, *49*, 5081.

(6) Golberg, D.; Bando, Y.; Kurashima, K.; Sato, T. *Scr. Mater*. **2001**, *44*, 1561.

(7) Rubio, A.; Myamoto, Y.; Blase, X.; Cohen, M. L.; Louie, S. G. *Phys. Rev. B* **1996**, *53*, 4023.

(8) Ajayan, P. M.; Iijima, S. *Nature* **1993**, *361*, 333.

(9) Tsang, S. C.; Chen, Y. K.; Harris, P. J. F.; Green, M. L. H. *Nature* **1994**, *372*, 159.

(10) Sloan, J.; Grosvenor, S. J.; Friedrichs, S.; Kirkland, A. I.; Hutchison, J. L.; Green, M. L. H. *Angew. Chem*. **2002**, *114*, 1204.

(11) Shelimov, K. B.; Moskovits, M. *Chem. Mater*. **2000**, *12*, 250.

(12) Guerret-Piecourt, C.; Le Bouar, Y.; Loiseau, A.; Pascard, H. *Nature* **1994**, *372*, 761.

(13) Bando, Y.; Ogawa, K.; Golberg, D. *Chem. Phys. Lett*. **2001**, *347*, 349.

(14) Han, W. Q.; Redlich, P.; Ernst, F.; Ruhle, M. *Appl. Phys. Lett*. **1999**, *75*, 1875.

(15) Tang, C. C.; Bando, Y.; Sato, T.; Kurashima, K. *J. Mater. Chem*. **2002**, *12*, 1910.

(16) Vaccarini, L.; Goze, C.; Henrard, L.; Hernandez, E.; Bernier, P.; Rubio, A. *Carbon* **2000**, *38*, 1681.

(17) Lourie, O. R.; Jones, C. R.; Bartlett, B. M.; Gibbons, P. C.; Ruoff, R. S.; Buhro, W. E. *Chem. Mater*. **2000**, *12*, 1808.

(18) Cumings, J.; Zettl, A. *Chem. Phys. Lett*. **2000**, *316*, 211.

(19) Laude, T.; Matsui, Y.; Marraud, A.; Jouffrey, B. *Appl. Phys. Lett*. **2000**, *76*, 3239.

(20) Tang, C. C.; Bando, Y.; Sato, T.; Kurashima, K. *Chem. Commun*. **2002**, *12*, 1290.

(21) Zhang, X. F.; Zhang, X. B.; Tendeloo, G. V.; Amelinckx, S.; Op de Beeck, M.; Landuyt, J. V. *J. Cryst. Growth* **1993**, *130*, 368.

(22) Massalski, T. B. *Binary Alloy Phase Diagrams*; ASM International: Materials Park, OH, 1992; p 2859.

(23) Goldstein, A. N.; Echer, C. M.; Alivisatos, A. P. *Science* **1992**, *256*, 1425.